The crystallization kinetics of low-molecular-weight polyethylene fractions

J. G. Fatou and C. Marco
Instituto de Ciencia y Tecnología de Polímeros, Juan de la Cierva 3, Madrid-28006, Spain

and L. Mandelkern
Department of Chemistry, and Institute of Molecular Biophysics, Florida State University, Tallahassee, Florida 32306, USA
(Received 28 July 1989; accepted 8 November 1989)

Overall crystallization rates of low-molecular-weight fractions of linear polyethylene have been measured. The molecular weights range from $M_N = 2900$ to $M_N = 11\,400$ and quantitative data were obtained in the temperature interval of 110 to 127°C, depending on the molecular weight. Crystallization kinetics obey nucleation theory appropriate to chains of finite length. Definite continuity is found between the kinetics of fractions with molecular weights greater than 8000 and high-molecular-weight fractions. The three lowest molecular-weight fractions appear to display some unique kinetic features. All the fractions display three distinct regimes and the transition temperature between regimes can be identified with characteristics in nucleation rates and do not correspond to an integral change in crystallite thickness.

(Keywords: crystallization kinetics; polyethylene; low-molecular-weight fractions; regimes; regime crystallization)

INTRODUCTION

The crystallization of long-chain molecules has been shown to be a classical nucleation-and-growth process with nucleation being the dominant factor in the region of the melting temperature[1]. A more detailed analysis of the crystallization process has shown the existence of different regimes as a function of the crystallization temperature[2]. As has been summarized previously, the existence of these regimes is a consequence of the different relations between the steady-state nucleation rate and the subsequent rate at which nuclei grow. Two extreme situations, regimes I and II, were initially considered for the case of non-chain low-molecular-weight substances[3,4] and subsequently adapted to polymers[5–7]. The situation at lower crystallization temperatures, i.e. large undercoolings, has also been described. The rate of nucleation is so high under these conditions that the concentration of nuclei is very dense and there is not sufficient space for lateral growth. This situation has been named regime III[8].

Other cases have also been considered. One is when the nucleus spreads out on the substrate[9]. The temperature coefficient is again the same as for regime I. Another situation is concerned with the relative rate at which chain units cross the nuclei–liquid interface. This physical situation differs from regime III and does not require a high nucleation rate, but the temperature coefficients are the same. According to these developments, the crystallization temperature coefficient exhibits breaks corresponding to the regime transitions. The analysis of the coherent surface nucleation of long-chain molecules has shown that the temperature coefficient slopes are in the ratio of 0.5 between regimes II to I, and the slope in regime III is the same as in regime I.

Experimental results for many polymers confirm the existence of regime I–regime II[10–15] and regime II–regime III transitions[16–21], but only in a few cases have the three regimes been observed in the same polymer system[22–24].

In the systems analysed, the experimental results appear to support the ratio 0.5 for the regime I–regime II transition. However, in a previous study with linear polyethylene fractions encompassing a very wide molecular-weight range, it has been shown that the influence of molecular weight on the regime behaviour is very profound. Three, two or one regimes are experimentally observed and the slope ratios of regime II/regime I, in those cases in which they are observed, are dependent on chain length[2]. There is a linear increase in this ratio with molecular weight. A ratio of unity is found in the limit of very high molecular weight.

The analysis given above has been limited to polymers of high molecular weight. The crystallization kinetics of low-molecular-weight fractions of several polymers have also been studied in detail, particularly polyethylene[10,25–27], poly(ethylene oxide)[28–31], higher polyoxides[32,33] and polysulphides[34,35]. Very recently, analyses of the high-molecular-weight n-alkanes concerned with crystallization kinetics have appeared[36,37]. Studies with these compounds allow a comparison of the characteristics of the alkanes with low-molecular-weight linear polyethylene.

The crystallization of low-molecular-weight polyethylene fractions and high-molecular-weight n-alkanes is of fundamental importance because, in this molecular-weight range, under appropriate crystallization conditions, it is possible to form crystallites whose thicknesses are comparable to the extended molecular length, although smaller sizes can also be developed.

Early studies on low-molecular-weight poly(ethylene oxide) resulted in many unusual results[28–31]. It has been shown that the growth rate *versus* crystallization temperature curves show at least one sharp break, and it has been proposed that the lamellar thickness changes with

0032-3861/90/050890-09
© 1990 Butterworth & Co. (Publishers) Ltd.

the crystallization temperature in a stepwise manner, assuming discrete values, and each part of the growth curve corresponds to a particular lamellar thickness[28,29]. Discrepancies with the kinetic theory have been discussed[38-40] and efforts have been made to develop new approaches[41,42]. A discontinuous change in overall crystallization rates has been observed in a very limited study of a low-molecular-weight polyethylene fraction[25]. The transition in the crystallization rate was supposed to be caused by the change of structure from folded-chain to extended-chain crystals. More recently, studies on crystallization kinetics in high-molecular-weight n-alkanes have been carried out for $C_{146}H_{294}$ and $C_{198}H_{398}$[36] and $C_{192}H_{386}$[37]. In this latter case, the experimental data follow the nucleation theory developed for chains of finite molecular weight and the same behaviour has been found for two low-molecular-weight polyethylene fractions. That is to say, there is no difference in the crystallization mechanism between the two types of samples.

In the present work we present and analyse the results of a study of the overall crystallization kinetics of a set of well characterized low-molecular-weight fractions of linear polyethylene. The molecular weights range from $M_N = 2900$ to $M_N = 11\,400$. The main purposes of the investigation were to assess whether there is a continuation of the crystallization process described previously for the higher molecular-weight fractions, to identify crystallization regimes and, if they exist, to locate the transitions between the regimes, their characteristics and the underlying basis for the regimes.

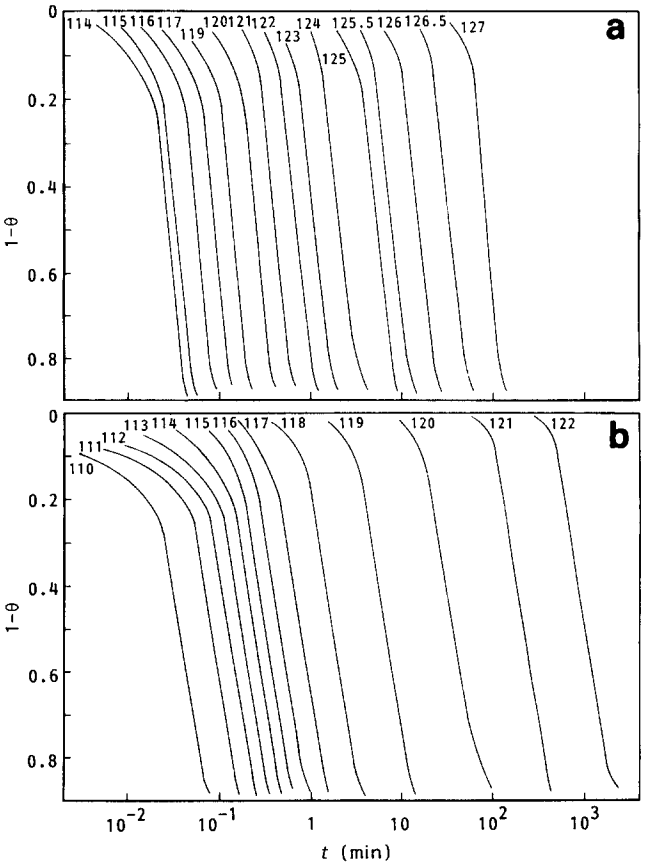

Figure 1 Logarithmic plot of $1-\theta$ against time for (a) $M_n = 11\,400$ and (b) $M_n = 2900$ at indicated temperatures

EXPERIMENTAL

Materials

Low-molecular-weight fractions, with M_N ranging from 2900 to 11 400, were used in this work. The characteristics of the fractions are given in *Table 1*.

Fraction A is a National Bureau of Standards (NBS) reference sample. Fractions B to E were obtained from Societé National Elf Aquitaine (SNEA) and the molecular weights of all these fractions were obtained by gel permeation chromatography.

Procedures

The crystallization kinetic studies were carried out by calorimetry. All d.s.c. measurements were made on a Perkin–Elmer DSC-7 differential scanning calorimeter. Automatic calibration was carried out with indium ($T_m = 156.60°C$, $\Delta H_u = 28.45\ J\ g^{-1}$) and zinc ($T_m = 419.47°C$, $\Delta H_u = 108.37\ J\ g^{-1}$) as standards.

The polymer samples, in amounts ranging from 3 to 10 mg, were placed in aluminium pans, weighed and crimped. The sample pan was then placed in the calorimeter holder and heated 20°C above the corresponding melting temperature for 10 min. These conditions ensured the complete melting of the sample and were used in all the experiments. Crystallization was carried out after cooling the sample from the melt at a rate of 64°C min^{-1}, until a given crystallization temperature was reached.

The exotherms were scanned as a function of time until no change in the d.s.c. energy axis was observed. The isotherms were obtained from the data points stored for each crystallization run on a Perkin–Elmer 7700 computer by using DSC-7 kinetic software.

Table 1 Molecular weights of polyethylene fractions

Fraction	M_n	M_w	M_w/M_n
A	11400	13600	1.19
B	8000	8400	1.05
C	5600	5800	1.04
D	3900	4000	1.03
E	2900	3100	1.07

RESULTS AND DISCUSSION

Crystallization kinetics

Crystallization kinetics from the pure melt were studied using the endothermic experiments described in the 'Experimental' section. Quantitative data were obtained in the temperature interval of 110 to 127°C, depending on the molecular weight of the sample. The crystallization times in this temperature range are of the order of about 0.1 to 10^4 min.

The general characteristics of the isotherms, for all molecular weights, are qualitatively very similar to those that have been reported previously for polyethylene fractions encompassing a very wide molecular-weight range[2,10]. *Figure 1* shows typical transformation–time plots for two fractions. A set of isotherms along the log time axis is observed. However, at the lowest crystallization temperatures, the initiation of crystallization is more poorly defined, probably as a consequence of the very fast onset of crystallization, within a time where thermal equilibrium is not reached.

The development of crystallinity with time has been described by Göler and Sachs[43] assuming that the evolution of a growing centre is independent of the mass transformed and of the growth of other centres.

For the initial portions of the transformation it is found that:

$$1-\lambda_t = Kt^n \quad (1)$$

where $1-\lambda_t$ is the crystallinity at time t, K is a constant and n defines the growth geometry.

The mutual impingement of growing centres upon one another was considered by Avrami[44] and the process is given by the equation:

$$1-\lambda_t = 1-\exp(-Kt^n) \quad (2)$$

Mathematically, equation (2) reduces in form to equation (1) for small extents of transformation. The Avrami exponent is thus the slope of the double logarithmic plot of $1-\lambda_t$ against t.

The agreement of the experimental data with the Avrami equation and the Göler–Sachs approximation is about the same, as was shown previously in the analysis of higher molecular-weight fractions[2,10].

Typical experimental results are plotted in *Figure 2*, according to the suggestion of equation (1). A linear relation is obtained for a significant portion of the total transformation and, for any given molecular-weight fraction, the slopes of the linear portions for the highest crystallization temperatures are found to be independent of temperature. The slopes of the straight lines are found to be 4. At lower crystallization temperatures, the slopes for molecular-weight fractions 2900, 3900 and 5600 are 3.

Previous studies[10] with low-molecular-weight polyethylene fractions also gave a slope of 4, when higher crystallization temperatures were used. However, changes of n from 3 to 4 with crystallization temperature have been found in low-molecular-weight samples[25]. A value of $n=4$, in a strictly formal sense, represents a homogeneous, or pseudo-homogeneous, nucleation process followed by three-dimensional growth.

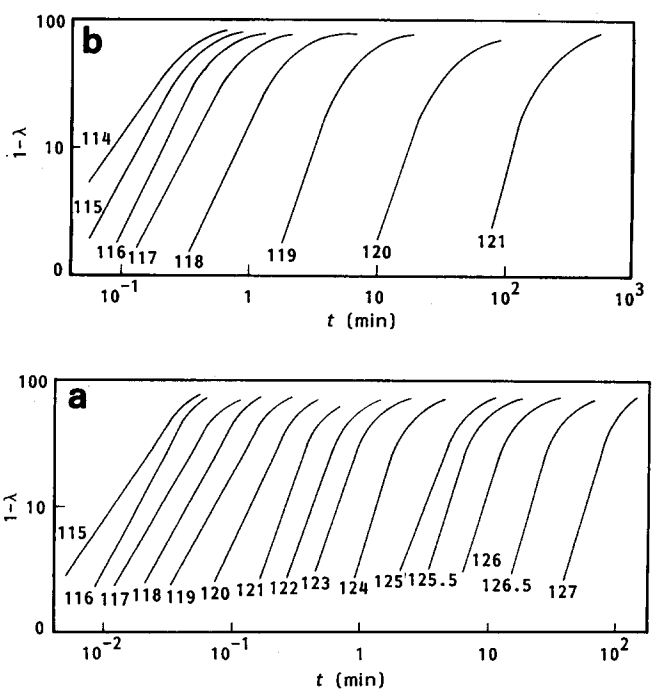

Figure 2 Double logarithmic plot of $1-\lambda$ against time for (a) $M_n=11\,400$ and (b) $M_n=2900$ at indicated temperatures

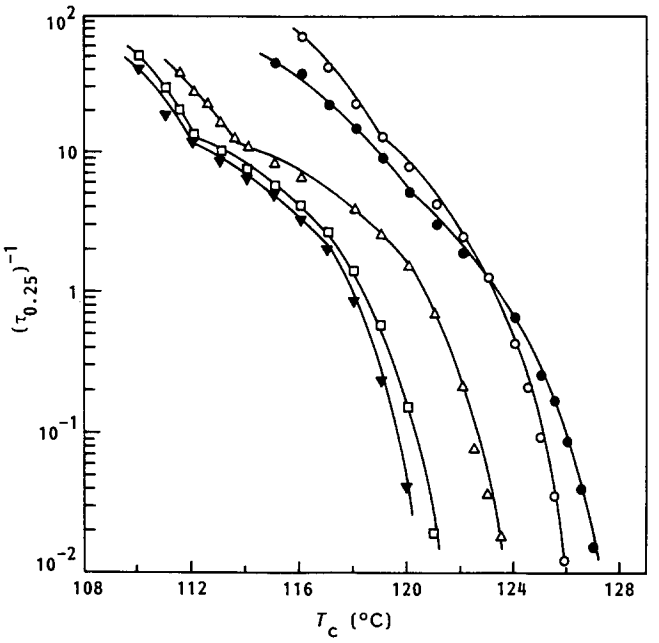

Figure 3 Plot of $\log(\tau_{0.25})^{-1}$ against crystallization temperatures for indicated molecular weights: (○) 1.14×10^4; (●) 8×10^3; (△) 5.6×10^3; (□) 3.9×10^3; (▼) 2.9×10^3

Another important observation is related to the level of crystallinity. Based on the enthalpy measurements, these low-molecular-weight fractions do not appear to be completely crystalline. The crystallinities range from 78% for the fraction $M_N=11\,400$ to 82% for the fraction $M_N=2900$.

For a given molecular weight, the experimental results for each temperature in the double logarithmic plot of $1-\lambda_t$ against time, after the deviations from linearity develop, form a common straight line of very small slope. This observation, previously reported[10], indicates that the levelling-off value of the degree of crystallinity is independent of the crystallization temperature.

Another interesting point is the influence of the crystallization temperature on the timescale of the crystallization process. This effect is very pronounced and *Figure 3* shows the plot of $(\tau_{0.25})$ against the crystallization temperature, $\tau_{0.25}$ being the time necessary to reach 25% of the transformation. The crystallization times increase over several decades as the crystallization temperature increases. Moreover, these plots exhibit a clear discontinuity at crystallization temperatures that depend strongly on molecular weight. For the three lower molecular weights, $M_N=2900$ to $M_N=5600$, the discontinuity temperatures are very close to one another and are in the range 112.0 to 113.5°C. The discontinuity temperatures for the two highest molecular weights, $M_N=8000$ and 11 400, are also very close to one another but at significantly higher temperature, 120.0 and 119.5°C, respectively.

Similar plots are also observed for the bulk crystallization kinetics of the n-alkane $C_{192}H_{386}$[37]. The growth rates of polyethylene fractions $M_N=2900$ and 3100, in dilute solution, show a very similar behaviour, while the fraction $M_N=11\,100$ does not display any discontinuity[26]. Low-molecular-weight poly(ethylene oxide) fractions, crystallized in the bulk, show comparable behaviour[30]. Therefore, we can conclude that the discontinuities such

as are observed in *Figure 3* are characteristic of the crystallization kinetics of low-molecular-weight chain molecules.

The final crystallite thicknesses that develop over this crystallization temperature range for the low-molecular-weight species are also of interest. The particular n-alkane studied always yields extended-chain crystals[37]. The dilute solution crystallization of the polyethylenes always gives a *continuous* decrease in the crystallite thickness with decreasing crystallization temperature over a temperature range that includes the discontinuity[26]. A continuous crystallite thickness–crystallization temperature function is also reported for low-molecular-weight poly(ethylene oxide) samples crystallized from dilute solution[45]. In the context of the polyethylenes studied here, it is well established for $M_N \gtrsim$ extended-chain length over the complete accessible range of crystallization temperatures[27]. Therefore, some type of folded-chain lamellar crystallite is formed for the higher molecular weights. However, the situation is quite different for the three lowest molecular weights. It has been reported[37] that, for fractions $M_N = 5600$ and $M_N = 3800$, extended-chain crystallites are formed at the higher crystallization temperatures, i.e. the crystallite thicknesses are comparable to the extended-chain length. However, as the temperature is lowered, there is a well defined interval of about 1–2°C where an abrupt decrease in the crystallite thickness is observed. This lower thickness, which decreases slowly with decreasing crystallization temperature, is not, however, an integral value of the extended-chain length. The situation for fraction $M_N = 2900$ can be assumed to behave in the same manner, a conclusion confirmed by our unpublished observation. This discontinuity in the crystallite thickness with crystallization temperature does not correspond to the discontinuity in the crystallization kinetics described by *Figure 3*. The values occur in fact 7–10°C higher. In contrast it has been reported that the discontinuities observed in the bulk crystallization of low-molecular-weight poly(ethylene oxide) correspond to integral changes in the crystallite thickness[28,29]. The relation of these discontinuities to regime kinetics will be discussed subsequently.

The influence of molecular weight on the timescale of the crystallization process is very pronounced. In *Figure 4*, the times $\tau_{0.25}$ as a function of molecular weight have been plotted at each of the crystallization temperatures. The rate data for higher molecular weights[2] are also included. There is continuity of the results from high to low molecular weights. It is very striking that for the lowest three or four molecular weights, depending on the crystallization temperature, the crystallization rates increase over several decades as the chain length increases. A maximum in the crystallization rate is reached. The molecular weight at which the rate achieves its maximum value is dependent on the crystallization temperature. For the lowest crystallization temperature it occurs at $M_N = 8000$. For the highest crystallization temperatures the maximum in the rate occurs at about $M_N = 2.5 \times 10^4$. There are then effectively two portions to the curves in *Figure 4*, implying rather strongly that different factors or mechanisms are involved in the crystallization process in the two different molecular-weight ranges. It should be noted that the low-molecular-weight region is that in which the free energy of nucleation is strongly dependent on chain length, as will be discussed later. Similar results to those described here were reported in an earlier work on the molecular-weight dependence of the crystallization kinetics of polyethylene[2].

Temperature coefficient

The crystallization rates display a very strong negative temperature coefficient, which is suggestive of a nucleation-controlled process. In its most general form, the

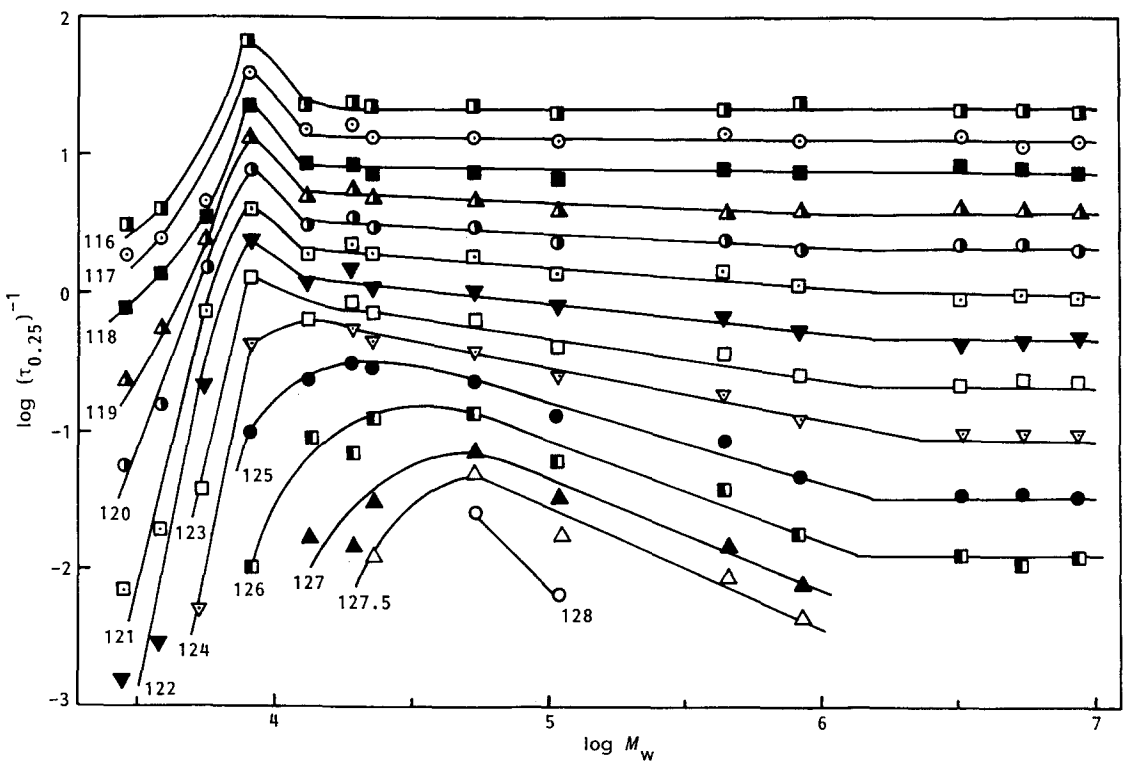

Figure 4 Plot of log $(\tau_{0.25})^{-1}$ against log M_n at indicated crystallization temperatures

steady-state nucleation rate N for all classes of molecular substances and nuclei types and shapes can be expressed as[46]:

$$N = N_0 \exp(-E_D/RT - \Delta G^*/RT) \quad (3)$$

where N_0 is a constant, E_D is the energy of transport in the solid–liquid interface and ΔG^* is the free energy of formation of a stable nucleus. Despite the important formalism of steady-state nucleation theory, there is a fundamental difference between low-molecular-weight, non-chain molecules and chain molecules including n-alkanes. The important distinction that is involved depends on whether the complete molecule or only a portion thereof participates in the formation of a nucleus. Clearly, chain molecules, even those of low molecular weight, do not participate in the formation of a nucleus. Therefore, the theory pertinent to chains of finite length needs to be employed. This problem has been treated for both three-dimensional homogeneous nucleation[47] and coherent two-dimensional nucleation[48] and can be extended to other types of nucleation processes.

From these, the critical dimensions for a three-dimensional nucleus are given by:

$$\rho^{1/2} = (2\sigma_u \pi^{1/2})/[\Delta G_u - RT/x - RT/(x-\xi^*+1)] \quad (4)$$

$$\xi^*/2[\Delta G_u - RT/x - RT/(x-\xi^*+1)] = 2\sigma_e - RT\ln[(x+\xi^*+1)/x] \quad (5)$$

$$\Delta G^* = \pi^{1/2}\xi^*\rho^{1/2}\sigma_u \quad (6)$$

In the nucleation by unimolecular deposition of chain sequences, the critical conditions are:

$$\rho^* = 2\sigma_u/[\Delta G_u - RT/x - RT/(x-\xi^*+1)] \quad (7)$$

$$\xi^* = [2\sigma_e - RT\ln(x-\xi^*+1/x)]/[\Delta G_u - RT/x] \quad (8)$$

$$\Delta G^* = 2\sigma_u \xi^* \quad (9)$$

In these equations, ρ^* is the number of lateral chains involved in the nucleus, ξ^* is the number of repeat units, σ_e and σ_u are the interfacial free energy per sequence as it emerges from the basal plane of the nuclei and the lateral interfacial free energy, respectively, x is the number of repeat units in the chains and ΔG_u is the free energy of fusion per repeat unit of the infinite chain, which can be approximated by the first two terms in a series expansion as:

$$\Delta G_u = \Delta H_u(T_m^\circ - T)/T_m^\circ \quad (10)$$

where T_m° is the equilibrium melting temperature of the infinite-size chain. It is important to note that the equilibrium melting temperatures of the finite-molecular-weight species are not involved in the formulation of the critical conditions and should not be used in the analysis. Equations (3) to (8) reduce, in the limit of high molecular weights, to the classical results for monomeric systems.

The analysis of the crystallization temperature coefficient can be carried out by equating the rate constant, expressed in terms of $(\tau_{0.25})^{-1}$, to the steady-state nucleation rate. The equilibrium melting temperature T_m° has been taken as $T_m^\circ = 145.5°C$[49].

The molecular weights that are considered in this work are in a range where ΔG^* changes dramatically with chain length. For this reason, nucleation theory for finite molecular weight has to be considered according to equations (3) and (9). For the calculation of the critical conditions, selected values of σ_e have been chosen. Reasonable values[50] appear to be in the range 1000–2500 cal mol^{-1}. These values have been used to calculate the values of $\Delta G/2\sigma_u T_c = \xi^*/T_c$, plotted in *Figure 5*. The data according to this analysis are very well represented by three intersecting straight lines. The characteristics of the plots are independent of the values taken for σ_e. Changing σ_e just shifts the data along the horizontal axis. The slopes of the straight lines are given in *Table 2* for each of the molecular weights. The straight lines representing the high- and low-temperature crystallization regions have, within experimental error, the same slope for the fractions $M_N = 5600$, $M_N = 3900$ and $M_N = 2900$. This is not the situation in the two highest molecular-weight fractions, $M_N = 8000$ and $M_N = 11\,400$. For these fractions the high- and low-temperature slopes differ significantly from one another and decrease with increasing molecular weight. In contrast, the slopes of the straight lines between the two temperature extremes are essentially constant with molecular weight. An important point is that the relative

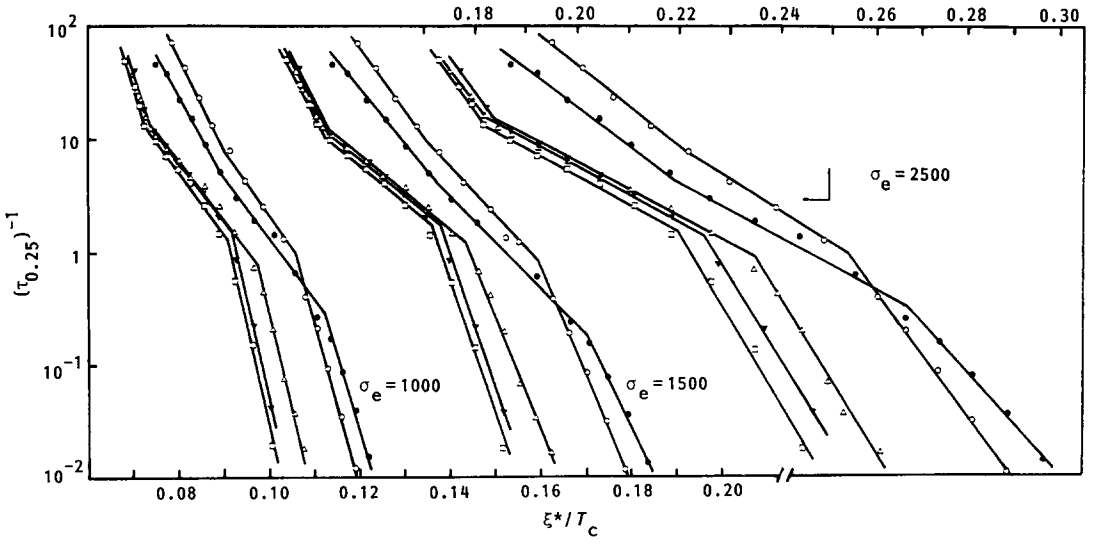

Figure 5 Plot of $\log(\tau_{0.25})^{-1}$ against ξ^*/T_c at indicated molecular weights: (○) 1.14×10^4; (●) 8×10^3; (△) 5.6×10^3; (□) 3.9×10^3; (▼) 2.9×10^3

Table 2 Slopes of the crystallization regimes for indicated σ_e values

	ξ/T_c											
	$\sigma_e=2500$			$\sigma_e=2000$			$\sigma_e=1500$			$\sigma_e=1000$		
M_n	III	II	I	III	II	I	III	II	I	III	II	I
11400	30.4	21.9	46.1	35.0	30.4	51.2	47.0	39.5	68.7	70.0	59.5	104.7
8000	31.5	23.8	54.8	40.8	32.8	66.8	52.2	43.6	92.3	83.5	64.8	138.5
5600	59.9	19.7	65.1	65.1	22.8	75.7	83.2	30.5	95.6	136.3	46.2	153.2
3900	56.8	23.5	63.1	81.6	29.2	90.7	112.8	36.1	124.0	169.4	57.0	186.2
2900	55.2	21.1	62.0	69.3	27.6	76.8	98.9	36.9	111.1	145.3	53.6	167.0

Table 3 Slope ratios between regimes for indicated σ_e values

	ξ/T_c											
	$\sigma_e=2500$			$\sigma_e=2000$			$\sigma_e=1500$			$\sigma_e=1000$		
M_n	II/I	II/III	III/I	II/I	II/III	III/I	II/I	II/III	III/I	II/I	II/III	III/I
11400	0.48	0.72	0.66	0.59	0.87	0.68	0.58	0.84	0.68	0.57	0.85	0.67
8000	0.43	0.76	0.57	0.49	0.80	0.61	0.47	0.84	0.56	0.47	0.78	0.60
5600	0.30	0.33	0.92	0.30	0.35	0.86	0.32	0.37	0.87	0.30	0.34	0.89
3900	0.37	0.41	0.90	0.32	0.36	0.90	0.31	0.34	0.91	0.31	0.34	0.91
2900	0.34	0.38	0.89	0.33	0.40	0.88	0.33	0.37	0.89	0.32	0.37	0.87

values of the slopes in each of the three regions are the same, irrespective of the σ_e values chosen.

The observation of three intersecting lines is suggestive of crystallization in different regimes, as observed in higher-molecular-weight fractions[2]. For the lower molecular weights, the crystallization at lower undercoolings can be assigned to regime I. As the crystallization temperature is lowered, the transition to regime II is clearly discerned. As the temperature is lowered further the sharp break in the slopes indicates regime III. The kinetic basis for the regime transition in the low-molecular-weight species is not necessarily the same as has been conventionally described for high molecular weights. The possible reasons for regime-type transitions in the crystallization kinetics of low-molecular-weight chain molecules has been discussed in detail previously[37].

In order to examine these points, the values of the ratios of the slopes are summarized in *Table 3* and plotted, as a function of molecular weight, in *Figure 6*. These ratios are effectively independent of the value of σ_e chosen. Also plotted in this figure are similar results for higher-molecular-weight fractions, which were obtained from several different sources[2,11]. As can be seen from *Figure 6*, the new data, for the lower molecular weights, join in a continuous manner those of the higher molecular weights. The molecular-weight dependence of the ratio for $M_N = 11\,400$ and $M_N = 8000$ is quite clear. From analysing both the table and the plot, the results for the three lowest molecular weights can be considered, within experimental error, either to continue this behaviour or to have reached a levelling-off value of about 0.3. There is at this stage not enough data in this very low molecular-weight range to enable an unequivocal decision to be made as to whether the slope ratios have reached an asymptotic value. If this state is reached it would indicate that there is a different crystallization mechanism for the three lowest molecular-weight samples. This possibility has already come up in our analysis of other aspects of the data. In the initial analysis of the coherent surface nucleation of polymers,

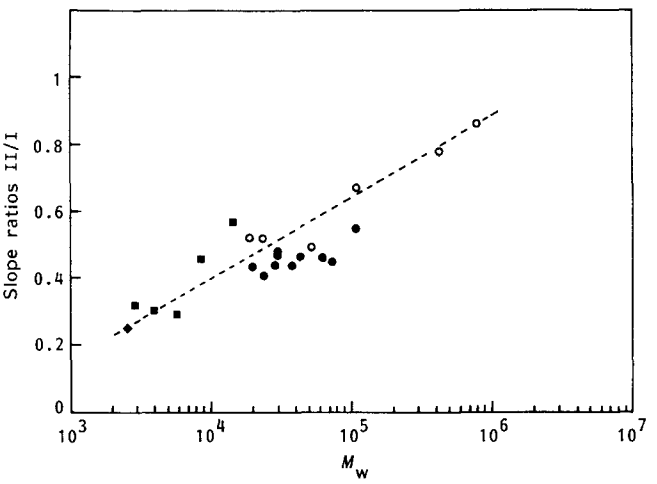

Figure 6 Plot of slope ratios II/I against molecular weight M_w: (●) ref. 11; (○) ref. 2; (◆) ref. 37; (■) this work

the temperature coefficient slopes were predicted to be in the ratio of 0.5 between regimes II and I[11]. Experimental results for many polymers appear to support this ratio. However, as is made clear in *Figure 6*, recent studies have shown that the influence of molecular weight on the regime behaviour is very profound[2]. As is indicated by the broken line in *Figure 6*, the slope ratios of regime I/regime II increase linearly with molecular weight. A value of unity is approached for very high molecular weights. This dependence of the slope ratios on chain length has been attributed to the molecular-weight dependence of the growth of nuclei[2]. As was pointed out, the ratio obtained here for the lowest molecular weights is approximately 0.3. Values of 0.23 to 0.25 have been found in the analysis of the crystallization kinetics of the high-molecular-weight n-alkane $C_{192}H_{386}$[37]. The value of this ratio falls on the broken line of *Figure 6*. It should be noted that in the original concept of regimes I and II, developed for

non-chain-like monomeric systems[3], the value of this ratio was calculated to be 0.33.

It is also of interest to examine the slope ratios between regimes III and I and between regimes II and III. In the former case, although the crystallization mechanisms are different in the two regimes, the slopes are expected to be the same[2]. This expectation is fulfilled, as is seen from the data in *Tables 2* and *3*, for the three lowest molecular weights, where the ratio is very close to unity. However, for the higher-molecular-weight fractions, $M_N = 11\,400$ and 8000, the ratios are reduced to the order of 0.6–0.7, for reasons that are not clear. These results are consistent with those previously reported for molecular weights of the order of 10^4. The slope ratios between regimes II and III behave similarly to those of the ratios between II and I. The values are constant for the three lowest molecular weights but increase with the two higher ones.

The previous analysis has been performed for two-dimensional coherent nucleation. The analysis can also be carried out for the three-dimensional nucleation process. We find that the major conclusions with regard to the regimes and their slopes are not altered in this analysis. We plot the rate data against the free energy of nucleation for finite chains, according to equation (6), for the nucleation mode (*Figure 7*). The general characteristics of these plots are the same as those described for two-dimensional nucleation. The values of the slopes for the three regions and the ratios of the slopes are summarized in *Table 4*. It should be emphasized that the

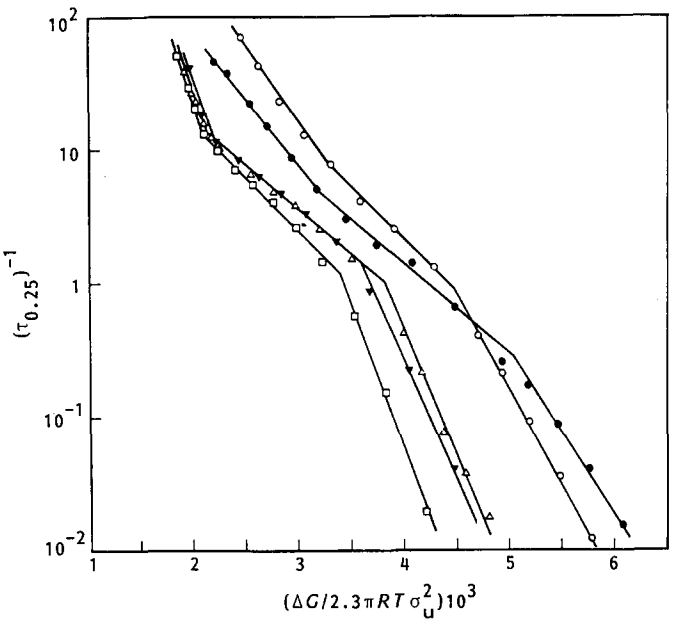

Figure 7 Plot of log $(\tau_{0.25})^{-1}$ against $\Delta G^*/2.3\pi RT_c\sigma_u^2$ at indicated molecular weights: (○) 1.14×10^4; (●) 8×10^3; (△) 5.6×10^3; (□) 3.9×10^3; (▼) 2.9×10^3

Table 4 Slopes and slope ratios for the three-dimensional process

	Slopes			Ratios		
M_n	III	II	I	II/I	II/III	III/I
11400	1022	677	1237	0.55	0.67	0.83
8000	1121	802	1442	0.56	0.72	0.76
5600	2050	645	1986	0.32	0.31	1.03
3900	2256	808	2200	0.36	0.36	1.03
2900	2150	706	1846	0.38	0.33	1.16

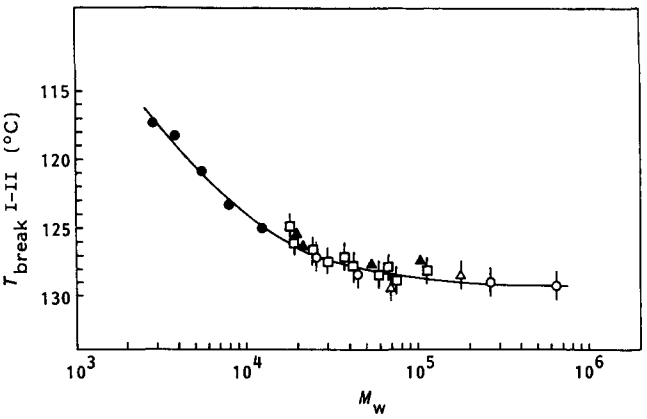

Figure 8 Plot of T_{I-II} against molecular weight: (▲) ref. 2; (○) ref. 10; (△) ref. 10; (□) ref. 11; (●) this work

agreement of the slope ratios with those described in *Table 3* is excellent, within experimental error, leading to the same conclusions as were discussed before. It seems, from this formal analysis, that the experimental data fit the functional forms required for either type of nucleation. This is a specific example of the more general principle that a variety of nucleation modes can be fitted to the same kinetic data. Consequently, a unique nucleation process cannot be deduced solely from the analysis of crystallization kinetics.

In addition to the observations of the regimes and the changes in slope that take place with molecular weight, the temperature of transition from one regime to another is also of interest. The transition temperature between regimes I and II, T_{I-II}, for two-dimensional nucleation, is plotted against the molecular weight in *Figure 8*. Data from the present work, from previous studies on higher molecular weights[2,10] and from the growth-rate studies[11] are included. This transition temperature is essentially independent of the value of σ_e chosen. The data for the lower-molecular-weight fractions are continuous with those for the higher molecular weight previously reported. However, there is clearly a very definite upswing to the data in the low-molecular-weight range. For example, T_{I-II} varies from 126°C for $M_N = 11\,400$ to 117°C for $M_N = 2900$. On the other hand, as has been noted previously[2,51], there is only a small but discernible change in T_{I-II} in the higher-molecular-weight range. These results strongly suggest a different mechanistic basis for regimes in the low-molecular-weight range. This conclusion is supported by the data for the transition temperature between regimes II and III, T_{II-III}, as is plotted in *Figure 9*. This transition temperature is also independent of σ_e. Here, except for the *three* lowest molecular weights, T_{II-III} does not differ by more than 1.5°C. However, for molecular weights less than 8000 there is a drastic decrease of about 9°C in T_{II-III}.

We can now compare the temperatures for the regime transitions T_{I-II} and T_{II-III} with other temperature discontinuities that have been observed in the crystallization behaviour of low-molecular-weight polyethylenes. Consequently we tabulate these data in *Table 5*. In the second column we give T_{disc}, the discontinuity temperature obtained from *Figure 3*. In the third and fourth columns we give the temperature range for the discontinuity in the melting temperature–crystallization plot that has been previously discussed. This temperature interval represents the transition from an extended-chain crystallite to a

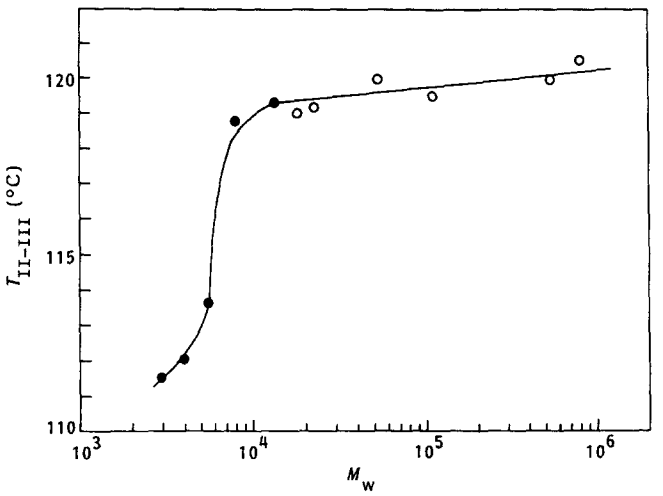

Figure 9 Plot of T_{II-III} against molecular weight: (○) ref. 2; (●) this work

Table 5 Temperature discontinuities (°C) in low-molecular-weight polyethylene fractions

M_n	T_{disc} [a]	$T_m - T_c$ [b]	$T_m - T_c$ [c]	T_{I-II}	T_{II-III}
2900	112.0	–	119–123	117.0	111.5
3900	112.0	121–122.5	120–122	118.5	112.0
5600	113.5	123–124	121–124	121.0	113.5
8000	120.0	–	–	123.5	119.0
11400	119.5	–	–	125.0	119.2

[a] From *Figure 3*
[b] From ref. [27]
[c] Unpublished work

non-integral, folded, lamellar crystallite[27]. The third column is from published reports for two samples that are virtually identical to those studied here[27]. The fourth column is from unpublished results from our laboratories. The last two columns give T_{I-II} and T_{II-III}, respectively.

From this tabulation we can see that the discontinuity in the crystallization rate obtained from *Figure 3* and the regime II–III transition temperature are in excellent agreement with one another for each fraction. These temperatures do not represent any major change in the relative crystallite thickness but rather a major change in the relative nucleation and growth rates[2]. Details of the basis for this regime transition in low-molecular-weight species have been given previously[37]. We see it manifested quite clearly in the crystallization kinetic data (*Figure 3*). In contrast we find that T_{I-II} does not exactly agree with the discontinuity in the $T_m - T_c$ plots. It is usually a few degrees lower, Hence, T_{I-II} does not represent a precise change in the relative crystallite thickness. In principle, this transition represents the temperature at which, subsequent to nucleation, a chain no longer grows rapidly into extended-chain crystallites[37]. Multiple nucleation events take place in regime II, which can then lead to reduced (non-integral) lamellar thicknesses, as is found in this regime for the three lowest fractions studied here. In contrast, although the n-alkane $C_{192}H_{386}$ displays a regime I–II transition, for the reasons cited above, extended-chain crystallites are formed over the complete range of crystallization temperatures. Thus, this transition in regimes does not necessarily have to result in a reduced crystallite thickness.

We have found that the overall crystallization kinetics of low-molecular-weight polyethylene fractions can be analysed in a formal manner when nucleation theory appropriate to chains of finite length is invoked. The kinetic data for molecular weights greater than 8000 follow a very similar pattern to that reported for very high molecular weights[2], so that a definite continuity is established. The three lowest molecular-weight fractions, $M_N = 2900$ to $M_N = 5600$, appear to display some unique kinetic features. All the fractions display regime transitions, which can be interpreted in the manner already delineated[2,37]. The transition temperatures between regimes can be identified with characteristics in nucleation rates and do not correspond to an integral change in crystallite thickness.

ACKNOWLEDGEMENTS

Support of the work at the Florida State University by the National Science Foundation Polymers Program Grant DMR 86-13007 is gratefully acknowledged. This work was also supported by the US–Spain Joint Committee for Scientific and Technological Cooperation and by CICYT, Madrid, Mat-88-0172, which are also gratefully acknowledged. The technical assistance of Mrs A. López Galán is also recognized.

REFERENCES

1 Mandelkern, L., 'Crystallization of Polymers', McGraw-Hill, New York, 1964
2 Fatou, J. G., Marco, C. and Mandelkern, L. *Polymer* submitted for publication
3 Hillig, W. B. *Acta Metall.* 1966. **14**, 1868
4 Calvert, P. D. and Uhlman, D. R. *J. Appl. Phys.* 1972, **43**, 1944
5 Sánchez, I. C. and Di Marzio, E. A. *J. Res. NBS (A)* 1972, **76**, 213
6 Lauritzen, J. I. *J. Appl. Phys.* 1973, **44**, 4353
7 Lauritzen, J. I. and Hoffman, J. D. *J. Appl. Phys.* 1973, **44**, 4346
8 Hoffman, J. D. *Polymer* 1983, **24**, 3
9 Sanchez, I. C. and Di Marzio, E. A. *J. Chem. Phys.* 1971, **55**, 893
10 Ergoz, E., Fatou, J. G. and Mandelkern, L. *Macromolecules* 1972, **5**, 147
11 Hoffman, J. D., Frolen, L. J., Ross, G. S. and Lauritzen, J. I. *J. Res. NBS (A)* 1975, **19**, 671
12 Alamo, R., Fatou, J. G. and Guzmán, J. *Polymer* 1982, **23**, 374
13 Vasanthakumari, R. and Pennings, A. J. *Polymer* 1983, **24**, 175
14 Allen, R. C., Ph.D. Dissertation, Virginia Polytechnic Institute and State University
15 Jadraque, D. and Fatou, J. G. *An. Quim.* 1977, **13**, 639
16 Clark, E. J. and Hoffman, J. D. *Macromolecules* 1984, **17**, 878
17 Monasse, B. and Haudin, J. M. *Colloid Polym. Sci.* 1985, **23**, 822
18 Pelzbauer, Z. and Galeski, A. *J. Polym. Sci (C)* 1972, **38**, 23
19 Dalai, E. N. and Phillips, P. J. *J. Polym. Sci., Polym. Lett. Edn.* 1984, **22**, 7
20 Barham, P. J., Keller, A. Otien, E. L. and Holmes, P. A. *J. Mater. Sci.* 1984, **19**, 2781
21 Lovinger, A. J., Davis D. D. and Padden, F. J. *Polymer* 1985, **26**, 1595
22 Phillips, P. J. and Vatansever, N. *Macromolecules* 1987, **20**, 2138
23 Lazcano, S., Fatou, J. G., Marco, C. and Bello, A. *Polymer* 1988, **29**, 2076
24 Monasse, B. and Haudin, J. M. *Makromol. Chem., Macromol. Symp.* 1988, **20/21**, 295
25 Sawada, S. and Mose, T. *Polym. J.* 1979, **11**, 227
26 Leung, W. M., Manley, R. St J. and Panaras, A. R. *Macromolecules* 1985, **18**, 760
27 Stack, G. M., Mandelkern, L. and Voig Martin, I. G. *Macromolecules* 1984, **17**, 321
28 Arlie, J. P., Spegt, P. and Skoulios, A. *Makromol. Chem.* 1967, **104**, 212
29 Kovacs, A. J. and Gonthier, A. *Koll. Z. Z. Polym.* 1972, **250**, 530

30 Kovacs, A. J., Straupe, C. and Gonthier, A. *J. Polym. Sci. (C)* 1977, **59**, 282
31 Kovacs, A. J. and Straupe, C. *Discuss. Faraday Soc.* 1979, **68**, 225
32 Marco, C., Fatou, J. G. and Bello, A. *Polymer* 1977, **18**, 1100
33 Marco, C., Fatou, J. G., Bello, A. and Blanco, A. *Polymer* 1979, **20**, 1250
34 Sánchez, A., Marco, C., Fatou, J. G. and Bello, A. *Makromol. Chem.* 1987, **188**, 1205
35 Sánchez, A., Marco, C., Fatou, J. G. and Bello, A. *Eur. Polym. J.* 1988, 24, 355
36 Ungar, G. and Keller, A. *Polymer* 1987, **28**, 1899
37 Stack, G. M., Mandelkern, L., Kröhnke, C. and Wegner, G. *Macromolecules* 1989, **22**, 4351
38 Point, J. J. and Kovacs, A. J. *Macromolecules* 1980, **13**, 399
39 Buckley, C. P. and Kovacs, A. J., in 'Structure of Crystalline Polymers' (Ed. T. H. Hall), Applied Science, London, 1983
40 Point, J. J., Colet, M. C. and Dosiere, M. *J. Polym. Sci., Polym. Phys. Edn.* 1986, **24**, 357
41 Hoffman, J. D. *Polym. Commun.* 1986, **27**, 39
42 Hoffman, J. D. *Macromolecules* 1986, **19**, 1124
43 Göler, V., Sachs, F. and Sachs, G. *Z. Phys.* 1932, **77**, 281
44 Avrami, M. *J. Chem. Phys.* 1939, **7**, 1103; 1940, **8**, 217
45 Pracella, M. *Eur. Polym. J.* 1985, **21**, 551
46 Turnbull, D. and Fischer, J. C. *J. Chem. Phys.* 1949, **17**, 71
47 Mandelkern, L., Fatou, J. G. and Howard, C. *J. Phys. Chem.* 1964, **68**, 3386
48 Mandelkern, L., Fatou, J. G. and Howard, C. *J. Phys. Chem.* 1965, **69**, 956
49 Flory, P. J. and Vrij, A. *J. Am. Chem. Soc.* 1963, **85**, 3548
50 Stack, G. M. and Mandelkern, L. *Macromolecules* 1988, **21**, 510
51 Allen, R. C. and Mandelkern, L. *Polym. Bull.* 1987, **17**, 473